Int. J. Heat Mass Transfer. Vol. 31, No. 7, pp. 1365–1374, 1988
Printed in Great Britain

0017–9310/88 $3.00 + 0.00

Natural convection heat transfer in an inclined porous layer

HIDEO INABA
Department of Mechanical Engineering, Kitami Institute of Technology, Koen-Cho 165, Kitami Hokkaido 090, Japan

MASAHIRO SUGAWARA
Department of Mechanical Engineering, Akita University, Tegata-Gakuen-Cho, Akita 010, Japan

and

JURGEN BLUMENBERG
Lehrstuhl C für Thermodynamik, Technishe Universität München, Augustenstr. 77 RgbI, D-8000 München, Federal Republic of Germany

(*Received* 8 *April* 1987 *and in final form* 1 *October* 1987)

Abstract—This paper reports an experimental study of natural convection heat transfer in an inclined rectangular cavity filled with liquid and spherical particles, in which two opposing isothermal walls are kept at different temperatures and other walls are thermally insulated. The experiments covered ranges of the modified Rayleigh numbers Ra^* from 34 to 3.8×10^4, inclination angles from 0° (heated below) to 180° (heated above), aspect ratios (height to width of the cavity) $H/W = 5$–32.7 and ratios of spherical particle diameter to width of the cavity $d/W = 0.074$–1.0. The non-dimensional correlation equations of the heat transfer rate across the porous layer were derived in functional relationships of the Nusselt number $Nu = cf$ (modified Prandtl number Pr^*, d/W, Ra^*, $\cos(\theta - 60°)$ or $\cos\theta$) for small inclination angles and $Nu = cf$ (Pr^*, H/W, Ra^*, $\cos(\theta - 60°)$ or $\sin\theta$) for large inclination angles. The functional relationship of inclination angle θ in the proposed correlation equations was determined for some ranges of the modified Rayleigh number.

INTRODUCTION

PHENOMENA of natural convection heat transfer in a porous layer have been observed in numerous environmental circumstances and used in some engineering fields. With regard to environmental circumstances, we note that natural convection has an important role in the temperature rise of underground water by geothermal energy, the diffusion of pollutants in the underground, the movement of moist air in the snow layer, etc. Among the engineering activities, natural convection heat transfer in the porous layer has been applied to sensible heat storage using porous media, porous insulation materials, the oil separation technique of oil sand by using steam and so on. Numerous fundamental researches have been undertaken in order to clarify the mechanism of natural convection in the porous layer using an enclosed rectangular cavity packed with liquid and spherical particles, in which two opposing walls are kept at different temperatures. Most of them have referred to the horizontal porous layer heated from below (inclination angle $\theta = 0°$) [1–6] and the vertical porous layer heated from the side wall ($\theta = 90°$) [7–10]. Vlasuk [11] and Holst and Aziz [12] investigated numerically natural convection heat transfer in a sloping porous layer. They predicted the existence of the maximum heat transfer rate at $\theta \cong 45°$–$60°$ in the range of modified Rayleigh numbers $Ra^* \leqslant 350$. Kaneko *et al.* [13] carried out experiments using some kind of sand in the range of $\theta \leqslant 30°$. Bories and Combarnous [14] reported the existence of a similar longitudinal coil flow with axes oriented up to the slope to that observed by Hart [15] in a pure fluid layer, from the visualization of the sloping porous layer in the range of $\theta = 15°$–$75°$ and $Ra^* = 40$–250. Most of the recent works mentioned above were performed in the limited range of parameters, e.g. $\theta \leqslant 90°$, $Ra^* \leqslant 800$, since the phenomena involve a lot of factors and it takes a long time to obtain the steady-state condition in experiments. Few researches have dealt with effects of a series of inclination angles from 0° (heated from below) to 180° (heated from above, without natural convection) via $\theta = 90°$ (vertical case) and a wide range of modified Rayleigh numbers on the natural convection heat transfer rate through an inclined porous layer.

The objective of this study is to obtain fundamental information related to the natural convection heat transfer rate through the inclined porous layer in wide ranges of parameters, that is, inclination angles, modified Rayleigh numbers, geometrical dimension of

NOMENCLATURE

a_m	thermal diffusivity of porous layer, $\lambda^*/(\rho c_p)_f$
c_p	specific heat at constant pressure
D	depth of porous layer (Z-direction)
Da	Darcy number, k/W^2
d	spherical particle diameter
g	gravitational acceleration
H	height of porous layer (X-direction)
H/W	aspect ratio
h	local heat transfer coefficient, $q/\Delta T$
h_m	mean heat transfer coefficient, $(1/H)\int_0^H h\,dx$
k	permeability, $(d^2/150)[\varepsilon^3/(1-\varepsilon)^2]$
Nu	mean Nusselt number, $h_m W/\lambda^*$
Pr^*	modified Prandtl number, ν_f/a_m
q	local heat flux, $q_{cv}+q_{cd}=q_T-q_{\theta=180^\circ}+q_{cd}$
q_m	mean heat flux, $(1/H)\int_0^H q\,dx$
q_T	total heat flux, $q_{cv}+q_{cd}+q_l$
$q_{\theta=180}$	total heat flux at $\theta=180^\circ$, $q_{cd}+q_l$
Ra	Rayleigh number, $g\beta\Delta TW^3/(\nu a_m)$
Ra^*	modified Rayleigh number, $Da\,Ra$
T	temperature
ΔT	temperature difference
W	width of porous layer (Y-direction)
X, Y, Z	coordinates.

Greek symbols

β	thermal expansion coefficient of fluid
ε	porosity
θ	inclination angle
λ	thermal conductivity of fluid
λ^*	effective thermal conductivity of porous media
ν	kinematic viscosity of fluid.

Subscripts

c, h	cold and hot walls, respectively
f	fluid
cd, cv, l	conduction, convection and heat loss
m	mean value.

spherical particles and rectangular cavity and physical properties of porous media. The obtained behavior of natural convection was explained from flow visualization through porous media, measurements of temperature profiles in the porous layer and results of heat transfer rate through the porous layer. In addition, non-dimensional heat transfer rates through the inclined porous layer were derived over wide ranges of the inclination angles and modified Rayleigh numbers.

EXPERIMENTAL APPARATUS AND PROCEDURE

The experimental apparatus mainly consisted of the heating part, cooling part and test part as depicted in Fig. 1. Four kinds of test section were constructed by inserting the lucite frame (15 mm thick) of 340 mm (fixed height H) × 10.4 mm (aspect ratio $H/W=32.7$), 22.5 mm ($H/W=15.1$), 34 mm ($H/W=10$) and 68 mm ($H/W=5$) (variable width W) section areas and 400 mm (fixed depth D) between the heating and cooling parts. The porous layer was formed by packing spherical particles and a liquid into the test section. A center part of 300 mm in depth (Z-direction) was used as the test section and both sides (50 mm length) of the test part in the Z-direction were used as the guard part. In order to obtain two opposing heating and cooling boundary conditions with a uniform temperature, the hot and cold walls (5 mm thick copper plate) were divided into three parts by 3 mm thick bakelite frames in the X-direction. The surface temperature of the hot wall was maintained at a uniform temperature using three main mica electric heaters (maximum output power of 1 kW). The guard mica

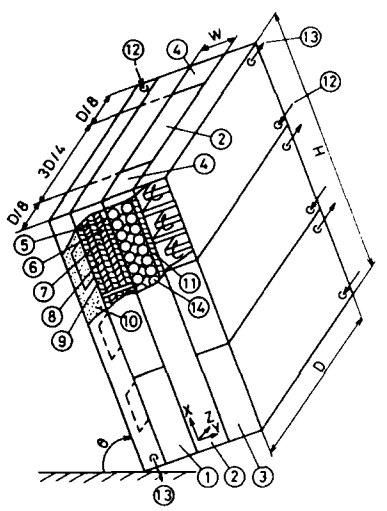

FIG. 1. Schematic diagram of the experimental apparatus.

heaters were mounted on the rear side of main heaters across a bakelite plate (5 mm thick) to minimize the heat loss from the main heaters to the environment. Consequently the surface temperature of the hot wall was controlled within ± 0.3°C at a given temperature. The surface temperature of the cold wall was kept at a uniform temperature by inducing coolant (brine) into each of three separate cooling chambers attached to the rear side of the cold wall. The surface temperature of the cold wall was controlled within ± 0.3°C at a given temperature. The fluid temperature distribution was measured using 15 copper–constantan thermocouples adhered to stainless steel pipes (0.8 mm in diameter), which were set at positions of $X = 85$, 170 and 255 mm, $D/2$ in the Z-direction and five positions determined in the Y-direction according to various widths of the porous layer. In order to minimize the heat loss from the experimental apparatus, the apparatus was covered with styro-foam insulation material 100 mm thick and placed in the temperature-controlled room. The heat loss from the experimental apparatus to the environment was ascertained to be less than $\pm 4\%$ by comparing the results of a horizontal porous layer heated from below ($\theta = 0°$) with the results reported by Schmidt and Silveston [16]. The experiments were made using three kinds of alumina balls of diameter $d = 5.1$, 10.2 and 22.2 mm, two kinds of glass beads of diameter $d = 5.03$ and 10.4 mm and iron balls of diameter $d = 9.5$ mm and water, ethyl alcohol and transformer oil. Their physical properties are listed in Table 1. Experimental data were taken after a steady-state thermal condition was reached. It took about 8–12 h to reach the steady-state condition. The physical properties in the non-dimensional variables were evaluated at the average of the surface temperatures of the hot and cold walls. The values of effective thermal conductivity of a porous medium were calculated from ten empirical correlation equations proposed by Kunii and Smith [17]. Other apparatus, similar to the apparatus mentioned above, was constructed to study visually the flow behavior of natural convection in the porous layer. The apparatus ($H = 110$ mm, $W = 22$ mm and $D = 110$ mm) was made of transparent material (lucite plate 10 mm thick) except the heating part. A porous layer was composed of distilled water and transparent glass beads ($d = 5.03$ mm). Flow behavior of liquid in the porous layer was visualized by tracing the movement of a red colored solution of potassium permanganate which appeared at various inclination angles of the porous layer. The present experiments were carried out using the following parameter ranges:

$$\text{porosity, } \varepsilon = 0.351\text{–}0.491$$

$$\text{aspect ratio, } H/W = 5\text{–}32.7$$

$$\text{modified Rayleigh number, } Ra^* = 34\text{–}3.8 \times 10^4$$

$$\text{modified Prandtl number, } Pr^* = 3.1\text{–}499.$$

EXPERIMENTAL RESULTS AND DISCUSSIONS

Temperature distribution in the porous layer

Figures 2(a)–(e) show typical fluid temperature distributions in the porous layer composed of water and glass beads ($d = 10.4$ mm) in the Y-direction for various inclination angles $\theta = 0°$, 60°, 90°, 120° and 150°, respectively, at the fixed positions of $X = 85$, 170 and 255 mm under the conditions of $H/W = 5$ ($W = 68$ mm) and temperature difference between the hot and cold walls $\Delta T = 28$°C. Typical temperature distributions for the case when $\theta = 0°$ (the heating of a horizontal porous layer from below) are presented in Fig. 2(a). It seems that these temperature distributions correspond with those of Bénard convection. The existence of the boundary layer flows in the horizontal direction along the hot and cold walls is presumed from the facts of the large temperature gradients in the vicinity of both walls and the small variation of temperature distribution in the center core region outside of both boundary layer flows in the Y-direction. Plural three-dimensional Bénard convections in the horizontal porous layer were also recognized by flow visual observation. The variation in temperature distribution for $\theta = 60°$ in Fig. 2(b) is independent of the distance X although those for $\theta = 0°$ are dependent on the distance X. The temperature difference of the porous layer between these measuring positions for $\theta = 60°$ becomes smaller than that for $\theta = 0°$ in Fig. 2(a). This behavior of temperature distribution for $\theta = 60°$ is caused by the existence of longitudinal coil rolls with axes directed up the slope reported by Bories and Combarnous [14]. These longitudinal coil rolls were also observed in the present study by visual observation of the liquid flow in the porous layer. Figure 2(c) presents the temperature distributions for $\theta = 90°$ (the heating of one vertical wall and the cooling of an opposing vertical wall). These results for $\theta = 90°$ show typical temperature distributions corresponding with a convective flow pattern of the vertical porous layer. That is, the decrease and increase in temperature gradients with an increase in X appear apparently in the vicinity of the hot and cold walls, respectively. These characteristics of the temperature gradient provide the existence of a boundary layer flow which ascends along the hot wall and descends along the cold one. As a result, a small variation in temperature appears in the center core region and the fluid temperature increases with increasing X in this center core region. The temperature distributions for $\theta = 120°$ are presented in Fig. 2(d). It is seen in Fig. 2(d) that small variations in temperature in the center region of the porous layer disappear. This indicates the reduction of the contribution of natural convection to overall heat transfer rate in the porous layer.

Effect of inclination angle θ on the average Nusselt number Nu

Figures 3(a) and (b) show the relationship between

Table 1. Physical properties of porous media used

	Specific weight ($kg\ m^{-3}$)	Specific heat ($kJ\ kg^{-1}\ K^{-1}$)	Thermal conductivity ($W\ m^{-1}\ K^{-1}$)	Thermal diffusivity ($m^2\ s^{-1}$)	Kinematic viscosity ($m^2\ s^{-1}$)
Water	998.2	4.180	0.594	1.42×10^{-7}	1.01×10^{-6}
Ethyl alcohol	790.0	2.415	0.183	9.55×10^{-8}	1.51×10^{-6}
Oil	866.0	1.892	0.124	7.58×10^{-8}	3.65×10^{-5}
Glass beads	2590	0.754	0.744	3.89×10^{-7}	—
Alumina balls	3560	0.837	1.593	5.34×10^{-7}	—
Iron balls	7830	0.461	53.45	1.47×10^{-5}	—

the average Nusselt number Nu and the inclination angle θ under the conditions of a combination of water–glass beads and aspect ratio $H/W = 5$ in the range of large modified Rayleigh number Ra^* and small Ra^*, respectively. In Fig. 3(a), the value of Nu increases with increasing inclination angle θ from 0° to about 60°, it has a maximum value of Nu at about 60°. The value of Nu decreases with an increase in θ in the case of $\theta > 60°$, and eventually the value of Nu becomes unity at $\theta = 180°$ which means the con-

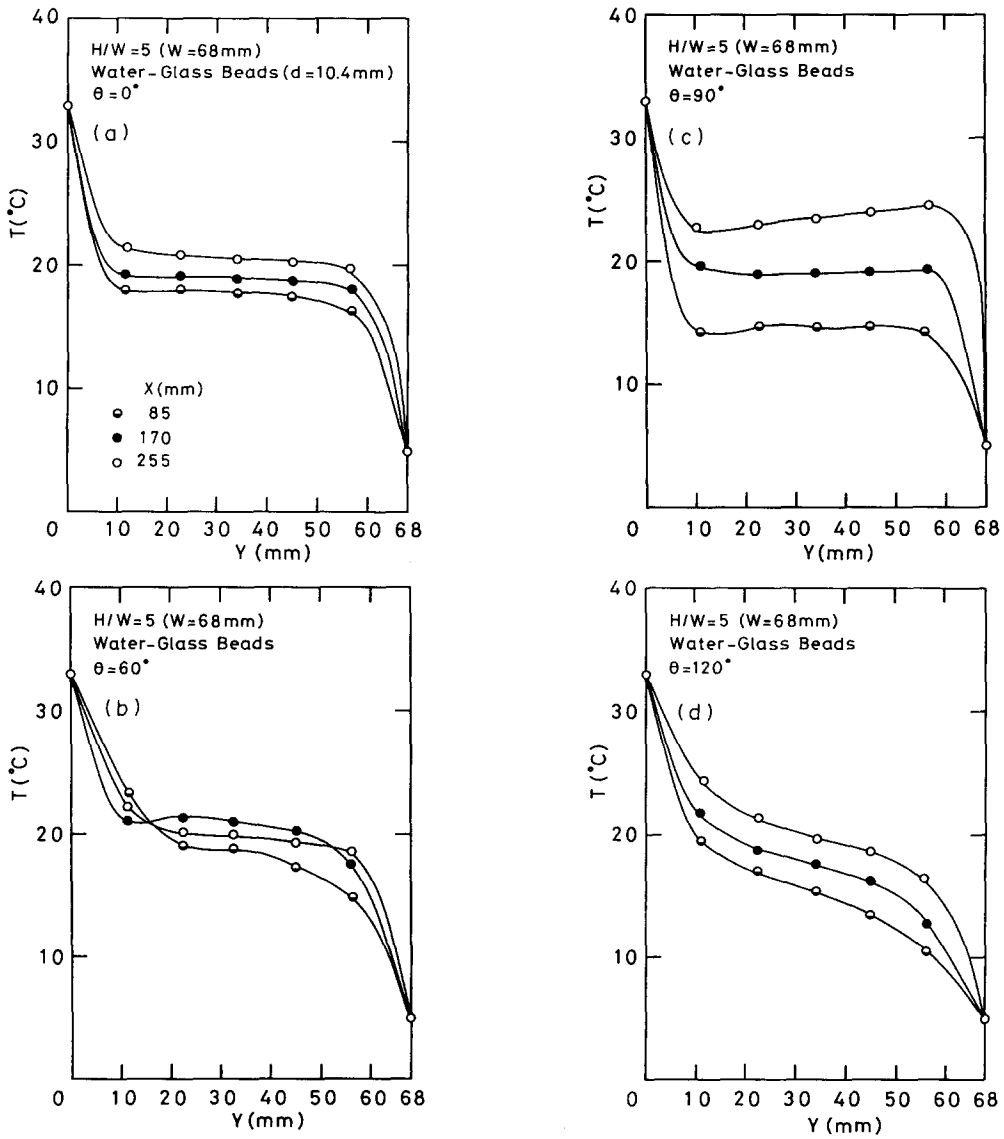

FIG. 2. Temperature distributions for $H/W = 5$, porous layer of glass beads saturated with water: (a) $\theta = 0°$; (b) $\theta = 60°$; (c) $\theta = 90°$; (d) $\theta = 120°$.

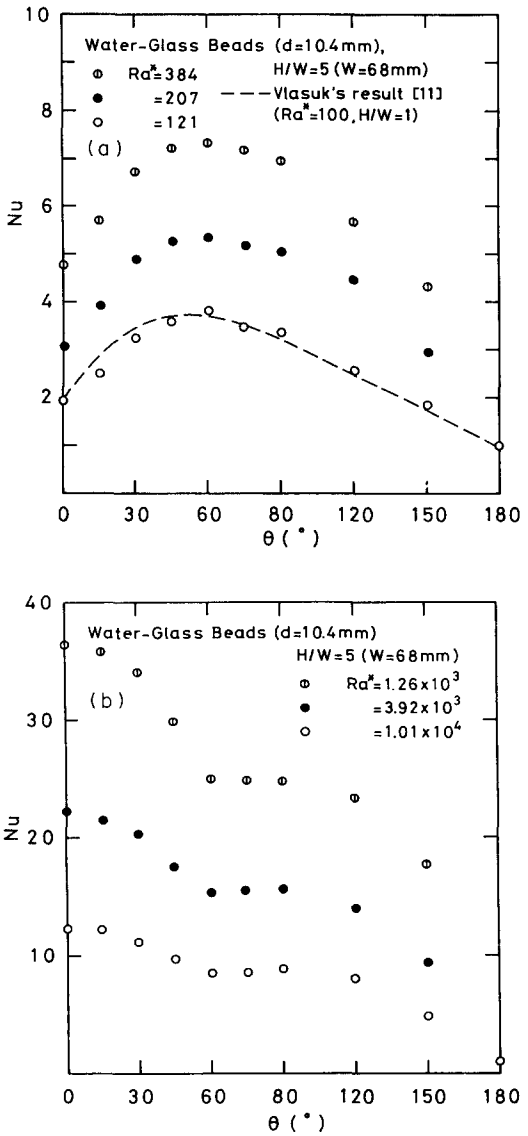

FIG. 3. Relationship between Nusselt number Nu and inclination angle θ: (a) for small modified Rayleigh number Ra^*; (b) for large modified Rayleigh number Ra^*.

ductive heat transfer through the porous layer without convection.

In Fig. 3(b) for a large modified Rayleigh number, a maximum value of Nu exists at $\theta = 0°$, the value of Nu decreases with an increase in θ from 0° to 60°, subsequently increases slightly with an increase in θ from 60° to 90° and for $\theta > 90°$ decreases as θ becomes large again. This behavior of Nu to θ for large Ra^* can be explained by the fact that the previous data of Nu at $\theta = 0°$ [1, 4] are larger than those at $\theta = 90°$ [7, 8], and also the heat transfer behavior in the inclined porous layer for large Ra^* is similar to that in the pure fluid layer [18], in terms of the marked contribution of the convective heat transfer for large Ra^*. It is seen that the value of Nu in the porous layer is dependent on various flow patterns according to the inclination angle θ, that is, the heat transfer through the porous layer at an inclination angle θ near 0° is mainly performed by Bénard cellular flow, and in the range of small inclination angles ($\theta > 0°$) the longitudinal coil flows observed by Bories and Combarnous [14] and in the present study predominate over the heat transfer in the porous layer. At around $\theta = 90°$, the heat transmission through the porous layer is mainly carried out by the boundary layer flows which appear in the vicinity of the hot and cold walls. Comparing the data for small Ra^* in Fig. 3(a) with those for large Ra^* in Fig. 3(b), one can note that the obtained data of Nu should be reduced according to the range of modified Rayleigh numbers Ra^*.

Effect of diameter of spherical particle and dimension of porous layer on the average Nusselt number

Figure 4(a) presents the variation of Nu with Ra^* for various ratios of the diameter of spherical particle to the width of the porous layer d/W and $\theta = 0°$. In Fig. 4(a), it is seen that the value of Nu decreases with an increase in d/W at a given Ra^*. This behavior of Nu to d/W agrees with the effect of d/W in the horizontal porous layer heated from below reported by Seki *et al.* [1]. This result reveals that the value of Nu should be derived by considering the effect of d/W on Nu for small inclination angles. The relation between Nu and Ra^* for various aspect ratios H/W and $\theta = 90°$ is shown in Fig. 4(b). In Fig. 4(b), it is noted that the value of Nu decreases with increasing H/W at a given Ra^*. This tendency of Nu to H/W is similar to the dimension effect of the porous layer on the heat transfer reported by Seki *et al.* [7] and Bories and Combarnous [14] in the experiment for $\theta = 90°$. The results indicate that aspect ratio H/W has an important role in estimation of the average Nusselt number for large inclination angles.

Effect of the physical properties of porous media on the average Nusselt number

Figure 5 shows the variation of Nu with Ra^* for various combinations between spherical particles and fluid under the conditions of $\theta = 0°$ and 90°. In Fig. 5, it is seen that the value of Nu increases with an increase in modified Prandtl number Pr^* at a given Ra^*. The present results coincide with those reported by Seki *et al.* [1, 7] and Schneider [8] who clarified the increase of Nu with increasing Pr^*. These results suggest that the data reduction of the heat transfer rate through the porous layer should include the effect of Pr^* except that the Pr^* is involved implicitly in the variable of Ra^*.

Non-dimensional correlation equations of the heat transfer through the porous layer

It was found that the Nusselt number representing non-dimensional heat transfer rate could be expressed with functions of inclination angle θ, ratio of spherical particle diameter to width of the porous layer d/W, aspect ratio H/W, modified Prandtl number Pr^* and

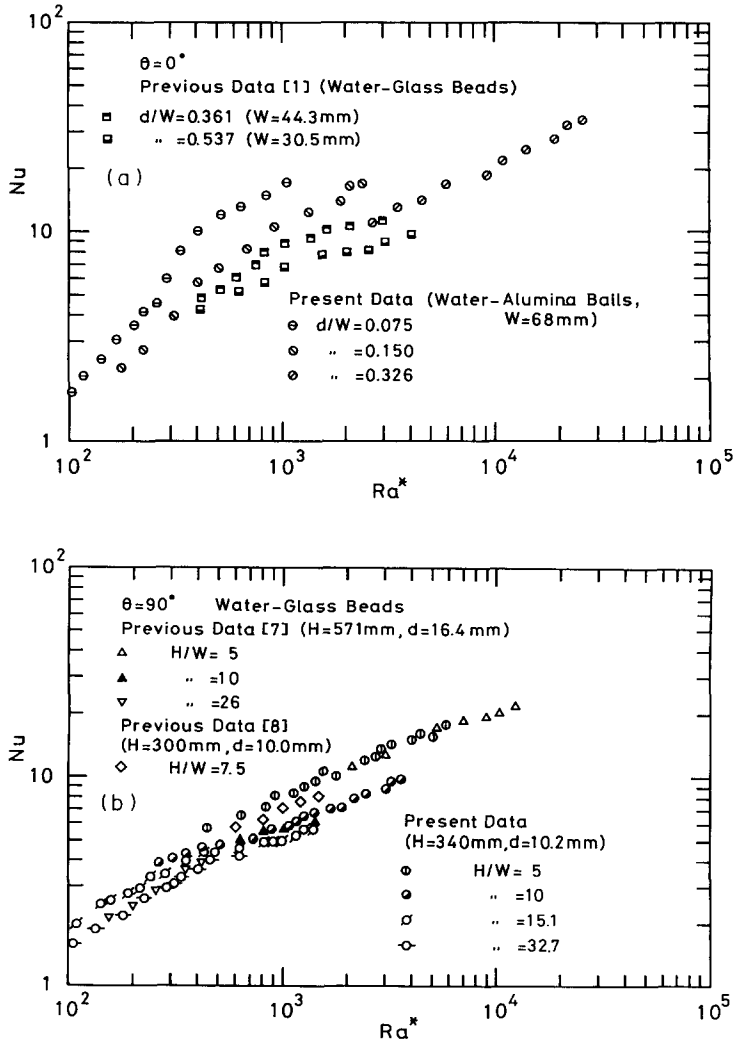

FIG. 4. Variation of Nu with Ra^*: (a) effect of ratio of spherical particle diameter to width of the porous layer d/W for $\theta = 0°$; (b) effect of aspect ratio of porous layer H/W for $\theta = 90°$.

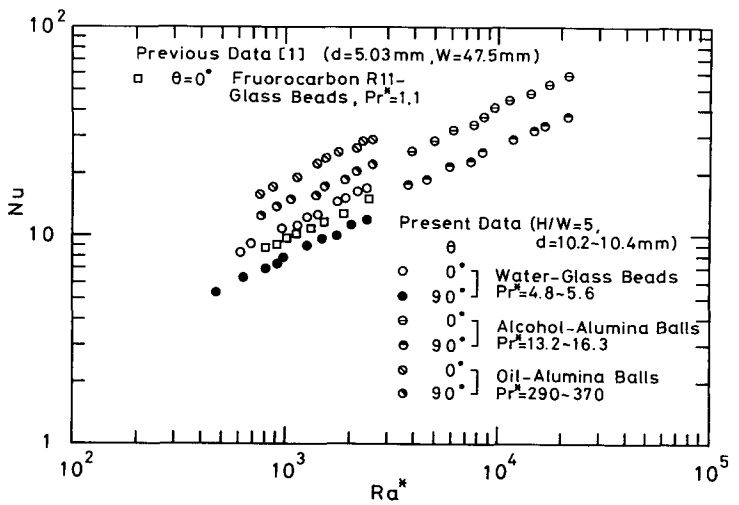

FIG. 5. Variation of Nu with Ra^* for various modified Prandtl numbers Pr^*.

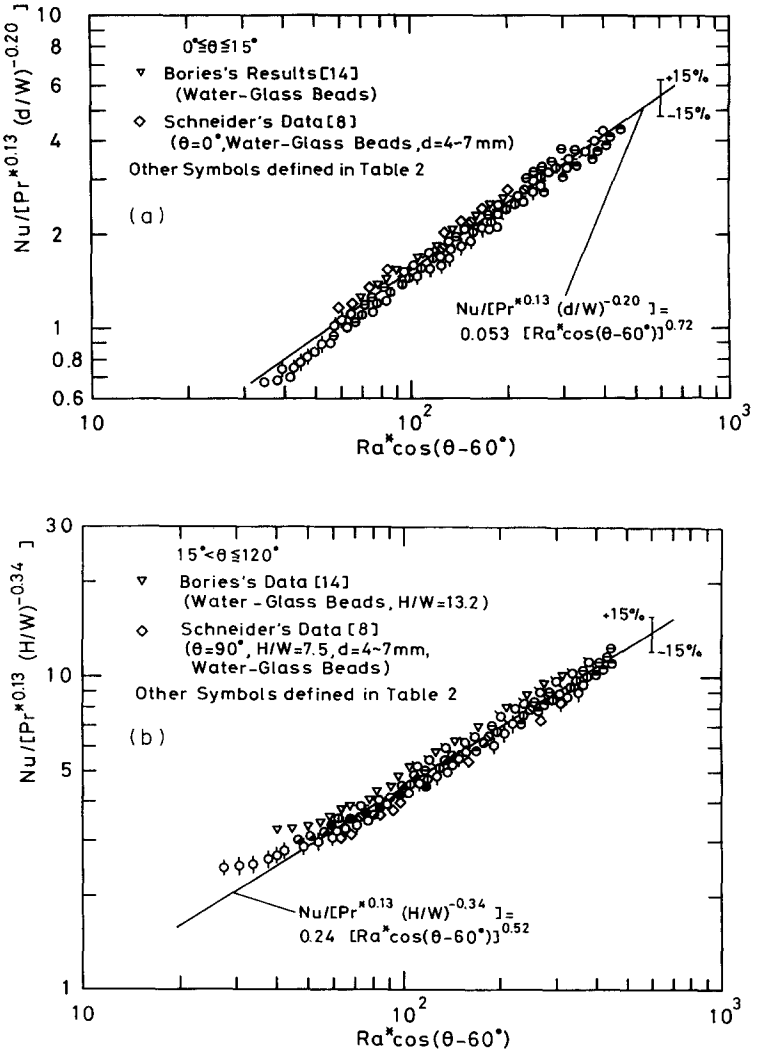

FIG. 6. Data reduction for small modified Rayleigh number Ra^*: (a) relationship between $Nu/[Pr^{*0.13}(d/W)^{-0.20}]$ and $Ra^*\cos(\theta-60°)$ for $0° \leqslant \theta \leqslant 15°$; (b) relationship between $Nu/[Pr^{*0.13}(H/W)^{-0.34}]$ and $Ra^*\cos(\theta-60°)$ for $15° < \theta \leqslant 120°$.

modified Rayleigh number Ra^* according to the ranges of θ and Ra^*. Therefore, it is possible to reduce the Nu data with the following functional relationships depending on inclination angle θ:

(1) for small inclination angle

$$Nu = cf\,(Pr^*, d/W, Ra^*, \theta); \tag{1}$$

(2) for large inclination angle

$$Nu = cf\,(Pr^*, H/W, Ra^*, \theta). \tag{2}$$

From equations (1) and (2), four empirical correlation equations (3)–(6) of average Nusselt number Nu are derived for Ra^* and θ over the ranges of $0.074 \leqslant d/W \leqslant 1.0$, $5 \leqslant H/W \leqslant 32.7$ and $3.1 \leqslant Pr^* \leqslant 499$, with some accuracy for the sake of simplicity using a least squares method.

(3) $60 \leqslant Ra^*\cos(\theta-60°) \leqslant 4.5\times10^2$,

$$0° \leqslant \theta \leqslant 15°$$

$$Nu = 0.053 Pr^{*0.13}(d/W)^{-0.20}[Ra^*\cos(\theta-60°)]^{0.72}. \tag{3}$$

Figure 6(a) presents plots of $Nu/[Pr^{*0.13}(d/W)^{0.20}]$ vs $Ra^*\cos(\theta-60°)$ for all data together with the data obtained by Bories and Combarnous [14] and Schneider [8]. This method of plotting data tends to bring the data together for different Pr^* and d/W. In Fig. 6(a), it is understood that equation (3) proposed in the present study is in agreement with the data with a standard deviation of $\pm 12.9\%$, although the data reported by Bories and Combarnous and Schneider are a little higher than that of equation (3).

(4) $60 \leqslant Ra^*\cos(\theta-60°) \leqslant 4.5\times10^2$,

$$15° \leqslant \theta \leqslant 120$$

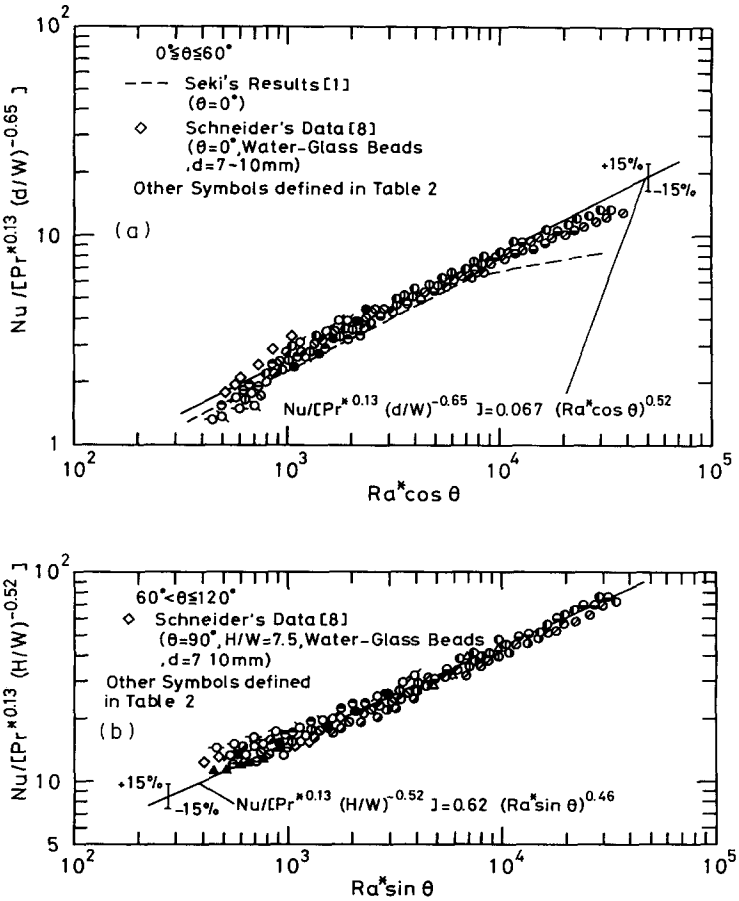

FIG. 7. Data reduction for large modified Rayleigh number: (a) relationship between $Nu/[Pr^{*0.13}(d/W)^{-0.65}]$ and $Ra^*\cos\theta$ for $0° \leqslant \theta \leqslant 60°$; (b) relationship between $Nu/[Pr^{*0.13}(H/W)^{-0.52}]$ and $Ra^*\sin\theta$ for $60° \leqslant \theta \leqslant 120°$.

$$Nu = 0.24Pr^{*0.13}(H/W)^{-0.34}[Ra^*\cos(\theta-60°)]^{0.52}. \quad (4)$$

In the present experimental ranges of d/W and H/W, the effect of d/W on Nu was too small to be expressed in equation (4). The data are plotted with the relationship between $Nu/[Pr^{*0.13}(H/W)^{-0.34}]$ and $[Ra^*\cos(\theta-60°)]$ in Fig. 6(b), together with the data reported by Bories and Combarnous [14] and Schneider [8]. The solid line (equation (4)) is consistent with the data with a standard deviation of $\pm 12.2\%$. On the other hand, for a large modified Rayleigh number Ra^*, the effect of inclination angle θ on the average Nusselt number can be represented by using $\cos\theta$ for a small inclination angle θ or $\sin\theta$ near $\theta = 90°$, since the behavior of θ to the average heat transfer rate for the porous layer is similar to that for a common fluid layer due to a large contribution of the convection to the overall heat transfer rate.

(5) $4.5\times10^2 \leqslant Ra^*\cos\theta \leqslant 3\times10^4$, $0° \leqslant \theta \leqslant 60°$

$$Nu = 0.067Pr^{*0.13}(d/W)^{-0.65}(Ra^*\cos\theta)^{0.52}. \quad (5)$$

Equation (5) is derived from all data with a standard deviation of $\pm 14.2\%$. Figure 7(a) shows plots of data with the relationship between $Nu/[Pr^{*0.13}(d/W)^{-0.65}]$ and $Ra^*\cos\theta$. In Fig. 7(a), the data for $\theta = 0°$ reported by Schneider [8] are slightly greater than the solid line of equation (5). The present correlation equation (5) agrees well with the results reported by Seki *et al.* [1] (dotted line) in the range of $Ra^*\cos\theta < 10^4$, but an increasing rate of $Nu/[Pr^{*0.13}(d/W)^{-0.65}]$ to $Ra^*\cos\theta$ for Seki *et al.*'s results becomes smaller than that of the present results for $Ra^*\cos\theta > 10^4$. It is intriguing that the effect of d/W on Nu for large Ra^* is more remarkable than that for small Ra^* as expressed in equation (3), comparing the exponents of d/W between equations (3) and (5).

(6) $4.5\times10^2 \leqslant Ra^*\sin\theta \leqslant 3\times10^4$, $60° < \theta \leqslant 120°$

$$Nu = 0.062Pr^{*0.13}(H/W)^{-0.52}(Ra^*\sin\theta)^{0.46}. \quad (6)$$

Figure 7(b) presents plots of $Nu/[Pr^{*0.13}(H/W)^{-0.52}]$ vs $Ra^*\sin\theta$. It is seen that all data including the data reported by Seki *et al.* [7] and Schneider [8] agree with the present correlation equation (6) within the maximum deviation of $\pm 13.1\%$. It is seen that comparing the exponents of H/W between equations (4)

Table 2. Explanation of symbols used in Figs. 6 and 7

Symbols	Solid (d, mm)	Fluid	d/W	H/W (H = 340 mm)
○	Glass beads (5.03)	Water	0.074	5
◍	Glass beads (10.4)	Water	0.153	
⊖	Alumina balls (5.10)	Water	0.075	
⊘	Alumina balls (10.2)	Water	0.150	
⊘	Alumina balls (22.2)	Water	0.326	
◓	Iron balls (9.50)	Water	0.139	
◒	Glass beads (10.4)	Ethyl alcohol	0.153	
◐	Alumina balls (10.2)	Ethyl alcohol	0.150	
◑	Alumina balls (10.2)	Oil	0.150	
◴	Alumina balls (22.2)	Oil	0.326	
◕	Glass beads (10.4)	Water	0.306	10
●	Alumina balls (10.2)	Water	0.300	
♀	Glass beads (5.03)	Water	0.224	15.1
♂	Glass beads (10.4)	Water	0.462	
♌	Alumina balls (10.2)	Water	0.453	
⊙	Glass beads (10.4)	Water	1.00	32.7

and (6), the effect of H/W exerts a greater influence on Nusselt number with an increase in Ra^*. In the present experimental range of parameters, the effect of d/W on Nu in the range of inclination angle near 90° is too small to be expressed as a function of Nu as can be seen in equations (4) and (6).

CONCLUSIONS

A study of natural convection heat transfer through an inclined porous layer bounded by two rigid isothermal boundaries kept at different temperatures has been carried out over the ranges of the inclination angle $\theta = 0°$–$180°$, ratios of spherical particle diameter to width of the porous layer $d/W = 0.074$–1.0, aspect ratios $H/W = 5$–32.7 and modified Rayleigh number $Ra^* = 34$–3.8×10^4. It was found that the natural heat transfer rate through the porous layer was influenced by flow patterns for the inclination angle: that is, three-dimensional Bénard cellular flows in a small inclination angle, longitudinal coil flow in the middle angle θ ($0° \leqslant \theta < 90°$), and boundary layer flow developing the hot and cold walls near $\theta = 90°$, which were observed by present visual observation of flow patterns and reported in ref. [14]. As a result of flow pattern, the existence of the maximum Nusselt number at around $\theta = 60°$ for small Ra^* or $\theta = 0°$ for large Ra^* was recognized in the present study. It was concluded that the contribution of d/W on Nu was remarked in a small θ and the contribution of H/W was significant near $\theta = 90°$, in relation to the geometric effect of the porous layer, and also the effect of those parameters on Nu varied in the range of modified Rayleigh number. Eventually it was concluded that the non-dimensional heat transfer rate through the inclined porous layer was derived with the functional relationship between Nu and $Ra^* \cos(\theta - 60°)$, $Ra^* \cos\theta$ or $Ra^* \sin\theta$ in some ranges of Ra^* and θ. Four kinds of non-dimensional empirical correlation equations were derived for Ra^* and θ.

Acknowledgements—The authors are very thankful to Mr T. Fukuda for his assistance in this experiment.

REFERENCES

1. N. Seki, S. Fukusako and Y. Ariake, Natural convection heat transfer in a horizontal porous layer having a relatively high Rayleigh number, *Trans. J.S.M.E.* **45**, 705–711 (1979).
2. T. Masuoka, Heat transfer by natural convection in a vertical porous layer, *Bull. J.S.M.E.* **24**, 995–1001 (1981).
3. J. W. Elder, Steady free convection in a porous medium heated from below, *J. Fluid Mech.* **27**, 29–48 (1967).
4. M. A. Combarnous and S. A. Bories, Hydrothermal convection in saturated porous media, *Adv. Hydrosci.* **10**, 231–279 (1975).
5. H. Robin, Heat dispersion effect on thermal convection in a porous medium layer, *J. Hydrol.* **21**, 173–185 (1974).
6. J. L. Robinson and M. J. O'Sullivon, A boundary-layer model of flow in a porous medium at high Rayleigh number, *J. Fluid Mech.* **75**, 459–467 (1976).
7. N. Seki, S. Fukusako and H. Inaba, Heat transfer in a confined rectangular cavity packed with porous media, *Int. J. Heat Mass Transfer* **21**, 985–989 (1978).
8. K. J. Schneider, Investigation of the influence of free thermal convection on heat transfer through granular materials, 11th Int. Congress Refrigeration, Paper No. II-4, pp. 247–253 (1963).
9. B. K. C. Chan, C. M. Ivey and J. M. Barry, Natural convection in enclosed porous media with rectangular boundaries, *J. Heat Transfer* **92C**, 21–27 (1970).
10. J. F. Weber, The boundary-layer regime for convection in a vertical porous layer, *Int. J. Heat Mass Transfer* **18**, 569–573 (1975).
11. M. P. Vlasuk, Heat transfer with natural convection in permeable porous medium, 4th All-Union Heat Transfer Conf., Minsk, Paper No. 1, pp. 49–54 (1972).
12. P. H. Holst and K. Aziz, A theoretical and experimental study of natural convection in a confined porous layer, *Can. J. Chem.* **50**, 233–241 (1972).
13. T. Kaneko, M. F. Mohtadi and K. Aziz, An experimental study of natural convection in inclined porous layer, *Int. J. Heat Mass Transfer* **17**, 485–496 (1974).
14. S. A. Bories and M. A. Combarnous, Natural convection in a sloping porous layer, *J. Fluid Mech.* **57**, 63–70 (1973).

15. J. Hart, Stability of the flow in a differentially heated inclined box, *J. Fluid Mech.* **47,** 547–576 (1971).
16. E. Schmidt and P. L. Silveston, Natural convection in horizontal liquid layers, *Chem. Engng Symp. Ser.* **55,** 163–169 (1959).
17. D. Kunii and J. M. Smith, Heat transfer characteristics of porous rocks, *A.I.Ch.E. Jl* **7,** 1–6 (1961).
18. H. Inaba, Experimental study of natural convection in an inclined air layer, *Int. J. Heat Mass Transfer* **27,** 1127–1139 (1984).

CONVECTION NATURELLE THERMIQUE DANS UNE COUCHE POREUSE INCLINEE

Résumé—On décrit une étude expérimentale sur la convection naturelle thermique dans une cavité rectangulaire inclinée remplie d'un liquide et de particules sphériques, pour laquelle deux parois opposées isothermes sont maintenues à des températures différentes et les autres parois sont thermiquement isolées. Les expériences couvrent des domaines de nombre de Rayleigh modifé Ra^* de 34 à $3{,}8 \cdot 10^4$, d'angle d'inclinaison de 0° (chauffage dessous) à 180° (chauffage dessus), de rapport de forme (hauteur sur largeur) $H/W = 5$–$32{,}7$ et de rapport diamètre de particule sphérique à largeur de cavité $d/W = 0{,}074$–$1{,}0$. Les formules adimensionnelles de flux de chaleur transféré à travers la couche poreuse sont $Nu = cf$ (nombre de Prandtl modifié Pr^*, d/W, Ra^*, $\cos(\theta - 60°)$ ou $\cos\theta$) pour des petits angles d'inclinaison et $Nu = cf$ (Pr^*, H/W, Ra^*, $\cos(\theta - 60°)$ ou $\sin\theta$) pour des grands angles. La fonction de l'angle d'inclinaison θ est déterminée pour quelques domaines du nombre de Rayleigh modifié.

WÄRMEUBERTRAGUNG DURCH FREIE KONVEKTION IN EINER GENEIGTEN PORÖSEN SCHICHT

Zusammenfassung—Diese arbeit berichtet über eine experimentelle Untersuchung auf dem Gebiet der Wärmeubertragung durch freie Konvektion in einem geneigten, rechteckigen Behalter, der mit Flüssigkeit und kugelförmigen teilchen (kugelschüttung) gefult ist. Dabei werden zwei gegeuberliegende isotherme Behälterwande auf unterschiedlichem Temperaturniveau gehalten, die anderen Behälterwande sind Wärmegedämmt (adiabat). Die Experimente wurden in folgenden Bereichen durchgeführt: Modifizierte Rayleighzahl Ra^* von 34 bis 3.8×10^4, Neigungswinkel θ von 0° (von unten beheizt) bis 180° (von oben beheizt), Streckungsverhaltnis (Höhe zu Breite des Behälters) $H/W = 5$ bis 32.7 und Verhältnis von Durchmesser der Schüttgutkugeln und Behälterbreite $d/W = 0.074$ bis 1.0. Die analytische Erfassung des eindimensionlen Wärmetransports durch die poröse Schicht des Behälters wurde durch die Korrelation mit der Nusseltzahl erzielt. Für Kleine Neigungswinkel gilt der Ansatz $Nu = cf$ (modifizierte Prandtlzahl Pr^*, d/W, Ra^*, $\cos(\theta - 60°)$ oder $\cos\theta$), für grosse Neigungswinkel gilt $Nu = cf$ (Pr^*, H/W, Ra^*, $\cos(\theta - 60°)$ oder $\sin\theta$). Die funktionelle Abhängigkeit des Neigungswinkels θ in der Korrelationsgleichung wurde an Hand der modifizierten Rayleighzahl bestimmt.

ЕСТЕСТВЕННОКОНВЕКТИВНЫЙ ТЕПЛОПЕРЕНОС В НАКЛОННОМ ПОРИСТОМ СЛОЕ

Аннотация—Экспериментально исследован естественноконвективный теплоперенос в наклонной прямоугольной полости, заполненной жидкостью и сферическими частицами, у которой две противоположные стенки поддерживаются при разных температурах, а две другие—теплоизолированы. Эксперименты проводились в диапазонах модифицированных чисел Рэлея Ra^* от 34 до $3{,}8 \cdot 10^4$, угла наклона от 0° (нагрев снизу) до 180° (нагрев сверху), отношения сторон (высота к ширине полости $H/W = 5$–$32{,}7$ и отношения диаметра сферической частицы к ширине полости $d/W = 0{,}074$–$1{,}0$. Безразмерные соотношения для расчета интенсивности теплообмена поперек пористого слоя получены в виде функциональных зависимостей числа Нуссельта Nu от модифицированного числа Прандтля Pr^*, d/W, Ra^*, $\cos(\theta - 60°)$ или $\cos\theta$ для малых углов наклона и от Pr^*, H/W, Ra^*, $\cos(\theta - 60°)$ или $\sin\theta$ для больших углов наклона. Функциональные зависимости от угла наклона θ в предложенных соотношениях определены для нескольких диапазонов модифицированного числа Рэлея.